ORIENTATION OF LIPID TUBULES BY A MAGNETIC FIELD

CHARLES ROSENBLATT, PAUL YAGER, AND PAUL E. SCHOEN
Francis Bitter National Magnet Laboratory, Massachusetts Institute of Technology, Cambridge, Massachusetts 02139; and Code 6190, Bio/Molecular Engineering Branch, Naval Research Laboratory, Washington, DC 20375-5000

ABSTRACT Lipid tubules, which are straight hollow cylinders consisting of lipid bilayers, are shown to orient in strong magnetic fields. Birefringence measurements were made of dilute samples of tubules of 1,2-bis(10,12-tricosadiynoyl)-sn-glycero-3-phosphocholine ($DC_{23}PC$) in magnetic fields of up to 4 T. The tubules were found to orient with their long axes parallel to the field direction, with saturated orientation ($\langle P_2 (\cos \theta) \rangle \gtrsim 0.95$) found at ~2 T. From known distributions of lengths and the number of bilayers in the walls, a value $\Delta\chi = (-7 \pm 1) \times 10^{-9}$ erg cm^{-3} G^{-2} was calculated for the tubules, which compares well with some previously reported values for phosphatidylcholines. Magnetic alignment will permit more sophisticated structural studies of monomeric and polymeric tubules, and provide a method of orienting macromolecules in the tubule walls or interior.

INTRODUCTION

It has been known for some time that biological membranes can be oriented by magnetic fields of 1 T or more. The first attribution of biomembrane orientation to the diamagnetism of constituent molecules was by Hong et al. (1971), who demonstrated that the summing of molecular interactions with the field was sufficient to orient retinal rod cells, and presented the formalism necessary for the interpretation of magnetic orientation of other membranous microstructures. In the case of the rod cells, the membrane proteins, and in particular their constituent alpha-helices, must account for much of the diamagnetic anisotropy.

Soon thereafter orientation of protein-free lipid bilayers by magnetic fields was reported by several independent groups (Gaffney and McConnell, 1974; Maret and Dransfeld, 1977; Boroski and Helfrich, 1978). Such orientation effects have been attributed to the weak anisotropic diamagnetism of the hydrocarbon chain, which results in the chains orienting perpendicular to a magnetic field (Londsdale, 1939). Often, however, liposomes, particularly multilayer liposomes, are polymorphic spherically symmetric structures and as such are not orientable. One might consider it surprising that such structures can exhibit an "orientation," although liposomes are sufficiently soft to permit an observable field-induced deformation of the spherical structure. The magnetic field–induced deformation and resulting optical properties of liposomes had earlier been worked out by Helfrich (1973).

The problem of measuring diamagnetic susceptibility anisotropies in relatively nondeformable liposomes was tackled by Boroske and Helfrich in 1978. Observing individual vesicles of egg lecithin under a phase-contrast microscope, they first determined the rotational diffusion constant D_r due to Brownian motion. Armed with a value of D_r, they switched on a magnetic field and measured the dynamic response of elongated vesicles to determine $\Delta\chi$, obtaining a value in cgs units of $-(0.28 \pm 0.02) \times 10^{-8}$ erg cm^{-3} G^{-2}. Nearly complete alignment of these prolate ellipsoids was obtained in 1.5 T, with the long axes parallel to the field. In a follow-up study Scholz et al. (1984) determined $\Delta\chi$ by observing the time-averaged orientational distribution function obtained from an elongated liposome in a weak field. For egg lecithin their value was 1.7× larger than the Boroske and Helfrich value, which they attributed to a compositional difference between the materials used in the two studies. In addition, they found a value of $\Delta\chi = -(0.96 \pm 0.1) \times 10^{-8}$ erg cm^{-3} G^{-2} for vesicles of dimyristoyl lecithin (DMPC). In all cases the lipids were in the fluid L_α phase. Using ^{31}P and deuterium nuclear magnetic resonance (NMR) as structural probes, Seelig et al. (1985) have confirmed if indirectly that at 7 T fluid protein-free liposomes orient with the normal to the bilayer perpendicular to the magnetic field. Seelig et al. were able to orient extracted bacterial lipids and a two-component mixture of unsaturated synthetic lipids when the hydrocarbon chains were fluid, but were, for unknown reasons, unable to orient samples of pure lipids.

The crystalline phase of lecithin was investigated by Sakurai et al. (1980, 1983), who studied the dynamic

Dr. Rosenblatt's current address is Department of Physics, Case Western Reserve University, Cleveland, OH 44106.

Dr. Shoen and Dr. Yager's current address is Bioengineering, FL-20, University of Washington, Seattle, WA 98195.

relaxation time of platelet crystals of the dihydrate dipalmitoyl phosphatidylcholine (DPPC) in the presence of a weak aligning magnetic field. The authors found the 0.1-mm-thick platelets to be diamagnetically biaxial, so that not only do the hydrocarbon tails orient perpendicular to the field, but the head groups, which lie in the plane of the platelets, orient perpendicular to the field as well. Their dynamic measurements yielded a value for $\Delta\chi$ of $\sim -9 \times 10^{-8}$ erg cm^{-3} G^{-2}, an order of magnitude larger than the L_α phase results discussed above. This difference was attributed to the higher degree of order in both the tail and head groups in the crystalline material. Nevertheless, these quantitative results must be viewed with considerable caution. In a biaxial material one expects two coupled rotational modes, each with a characteristic decay time, whereas Sakurai et al. measured a single average characteristic time. Moreover, Sakurai et al. simply measured light transmission through two crossed polarizers without formally relating the measured intensities to platelet orientation. Finally, they did not account for the distribution in platelet dimensions; since the rotational friction coefficient scales as length cubed, a distribution in platelet size can result in severe errors in the susceptibility (Lewis et al., 1985). (In contrast, Boroske and Helfrich observed individual vesicles using optical microscopy, independently measuring, rather than calculating the rotational diffusion coefficient.)

A new type of lipid microstructure has recently been discovered which consists of lipid bilayers wrapped around a hollow core. This structure, which we call a tubule, can be formed by polymerizable diacetylenic phosphatidylcholines (Yager and Schoen, 1984; Yager et al., 1985; Singh and Schnur, 1985; Singh et al., 1986; Georger et al., 1987). The lecithin 1,2-bis(10,12-tricosadiynoyl)-sn-glycero-3-phosphocoline ($DC_{23}PC$), for example, contains two diacetylenic groups in the middle of each hydrocarbon chain that render it and similar lipids polymerizable (Johnston et al., 1980; Hupfer et al., 1981; O'Brien et al., 1981; Albrecht et al., 1982; Lopez et al., 1982; Leaver et al., 1983; Schoen and Yager, 1985). The tubules can be perfectly straight and are ~0.75 μm in diameter, tens or even hundreds of micrometers in length, and have walls that vary from 1 to ~10 bilayers in thickness (see, for example, Yager et al., 1985). Diacetylenic lipid tubules form in two ways: they will grow by conversion of liposomes as the hydrocarbon chains in the liposomes crystallize at their characteristic phase transition temperature (Yager and Schoen, 1984; Yager, P., R. R. Price, J. M. Schnur, P. E. Schoen, D. Rhodes, and A. Singh, manuscript submitted for publication), or by precipitation of a solution in organic solvent by addition of a nonsolvent such as water (Georger, et al., 1987). Similar structures have also been formed from a very different lipid that is charged, nonpolymerizable, and has a natural amino acid as its chiral center (Nakashima et al., 1985).

The bilayers in tubules are all parallel to the long axis, so such a structure should orient in a magnetic field. However, little is yet known of the conformation or packing of the lipid molecules within the tubule walls. A correlation between the molecular orientation and that of the tubule as a whole is implied by coherent linear dichroism of the polymer along the entire length of the tubules, but there is no crystallographic data to support this hypothesis. We report the results of our exposure of dilute suspensions of tubules to high magnetic fields, using birefringence to determine the degree of alignment.

MATERIALS AND METHODS

The lipid 1,2-bis(10,12-tricosadiynoyl)-sn-glycero-3-phosphocoline ($DC_{23}PC$) was synthesized according to previous published methods (Johnston et al., 1980) and was purified to a single spot by thin-layer chromatography. Tubules were prepared by dissolution of the lipid in ethanol to 0.5 mg/ml, followed by addition of 50% triple distilled water by volume at room temperature, which produces a precipitate that consists primarily of tubules (Georger et al., 1987). Samples to be polymerized were then dialyzed to 20% ethanol, cooled to 0°C, and polymerized to a dark red color by exposure to 5.5 Mrad of ^{60}Co gamma radiation. Both monomeric and polymerized tubules were then dialyzed three times against 2,000 vol of triple distilled water for a total of over 18 h to remove residual ethanol. Data presented here are from polymerized tubule samples.

To obtain the distribution of tubule lengths a small amount of sample was placed between a microscope slide and coverslip. Several photographs of the sample were taken using an Olympus BHA microscope (Olympus, Tokyo, Japan) in phase-contrast mode. The length distribution, shown in Fig. 1, was obtained from optical micrographs of 101 individual tubules, where the mean length was found to be 21 ± 7 μm.

The distribution of the number of bilayers in the tubule walls was determined as follows using electron microscopy. When suspensions of thin tubules prepared as described are dried in air, the tubules flatten to produce 1-μm-wide strips. As a single bilayer is sufficiently electron dense to be resolved, the number of layers in the tubule wall can be counted. Tubules were dried on a carbon film–coated copper grid and placed in the upper stage of a DS-130 scanning electron microscope (International Scientific Instruments Inc., Santa Clara, CA) equipped with a model 9000 image processing system (Kevex Corp., Foster City, CA). The instrument was operated in the scanning transmission mode and a digitized image was recorded (dynamic range of 256). The magnification was such that several dozen non-overlapping tubules could be seen in a single image (Fig. 2), and tubules were ~5-pixels wide to assure that at least two pixels along a line perpendicular to the tubular axis reflected the true electron density.

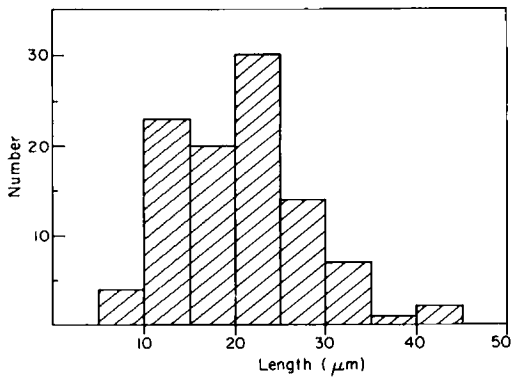

FIGURE 1 Length distribution based upon a sample of 101 tubules.

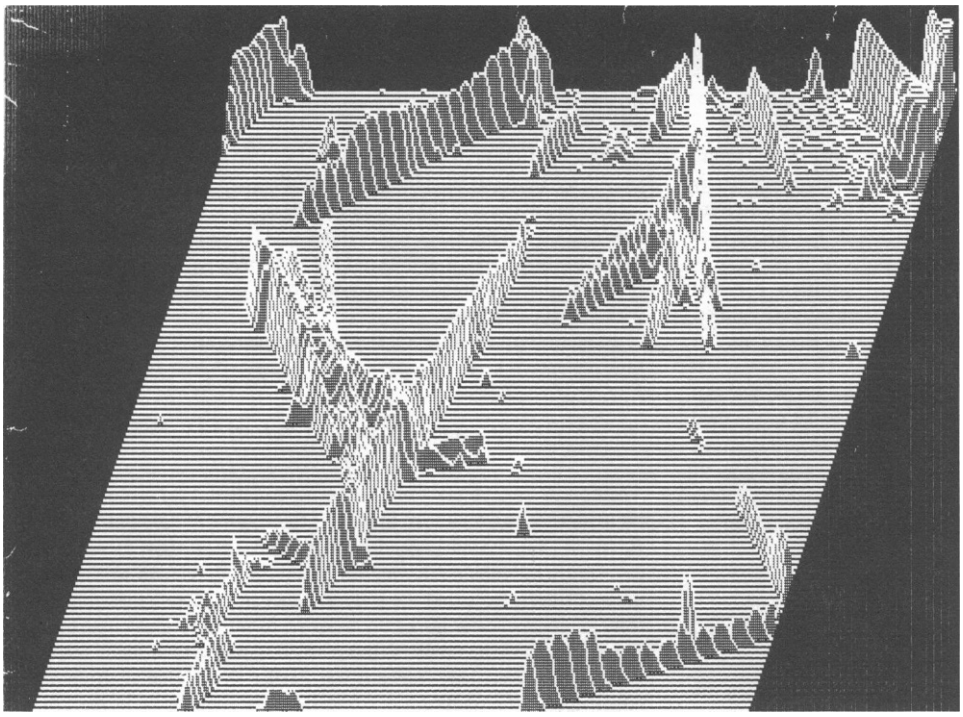

FIGURE 2 A pseudo three-dimensional plot created from an image of a field of tubules on a thin carbon support recorded in STEM mode. The height of peaks above the plane reflects the intensity of electron scattering by tubules at each point, which is presumed to be linearly proportional to the number of lipid bilayers in the tubule walls. Note that the thickness of a tubule wall is often not constant along its entire length.

In the scanning transmission mode each bilayer in a tubule wall can be assumed to contribute equally to reducing the electron beam intensity. Absorbance, which should be proportional to the number of bilayers in the wall is, according to Beer's law, $\log(I/I_0)$. The copper grid was chosen as an electron opaque standard (just above zero counts), and the background intensity of electrons passing through the carbon support was adjusted to just below 255 counts, or I_0. The image was color-coded such that six different colors corresponding to differentiable electron densities were created. Care was taken that the first discrete level that differed from the background included only the least dense complete tubules. These were presumed, based on high-magnification images, to have walls consisting of a single bilayer. If, however, walls were quantized in bilayer pairs, such as 2, 4, 6, etc., then all subsequent volume susceptibility results would be two low by a factor of two; we feel, however, that this is an extremely unlikely possibility. The numerical boundaries of other categories were chosen to give the longest stretches of uniform color along individual tubules.

As individual tubules were often of different thicknesses along their lengths, we chose to measure the total length of non-overlapping tubular material of a particular color, which corresponds to the distribution in wall thickness. It was also assumed that only even numbers of bilayers would be observed in complete tubules. The data are presented in Table I.

Magnetic Birefringence Measurements

The tubule suspension was diluted to a concentration of 0.17 mg/ml and placed in a stoppered glass cuvette having a 1-cm optical pathlength. The cuvette was housed in a cylindrical brass oven maintained at 27 ± 0.2°C, and in turn situated in the bore of an 11.2-T Bitter magnet possessing a transverse optical port. The sample was illuminated by a He-Ne laser (Model 124B; Spectra Physics Inc., Mountain View, CA) attenuated to ~0.8 mW.

Field induced birefringence was measured by means of an automatically compensating Pockels cell modulated at 2,800 Hz. The apparatus is described in detail (Rosenblatt, 1984). Although sensitivity for the device is better than $\Delta n \sim 10^{-9}$, much larger noise fluctuations ($\sim 3 \times 10^{-8}$) were observed, ostensibly due to the sample itself; thus it was often difficult to precisely establish the zero birefringence, which ultimately led to an experimental run-to-run variation in tubule susceptibility anisotropy of some ±15%. The possible origins of the apparently random baseline drift are several, including shear induced orientation caused by tubule sedimentation, clustering of tubules, and small convection currents in the sample. Note that more concentrated and more dilute samples were also used, with a corresponding increase and decrease in absolute noise, but little observable change in the signal-to-noise ratio.

With the sample in place, the field was increased step-wise from 0 to 4

TABLE I

Arbitrary color code	Counts	Total length*	Absorbance		Wall thickness in bilayers
			Range	Mean	
White	255–258	Background	0.0–.005	0.002	0
Red	227–184	25.2	0.005–0.14	0.1	1
Yellow	183–143	51.4	0.14–0.25	0.2	2
Green	142–99	56.0	0.025–0.41	0.33	3
Blue	98–50	16	0.41–0.71	0.56	4–7
Purple	49–1	2.5	0.71–very large		>7
Black	0	Grid bar	Infinity		

*In arbitrary units. The errors in these values are ±1 unit.

T (1 T = 10 kG). Typically 2–3 min were required before the orientational distribution equilibriated at each field setting, particularly when the magnetic field was small. The birefringence, as determined by the compensating voltage applied to the Pockels cell, was recorded at each step, and the field subsequently increased. Before beginning a new field sweep, the birefringence was allowed to decay at zero field for ~25 min, i.e., for more than 10 τ, where τ is the characteristic orientational decay time of a rigid rod of average length. Several such sweeps of the field were thus performed. (During preliminary measurements it was found that upon switching off the field the birefringence did not decay monotonically to zero, but rather exhibited a small "bump" of duration 1 τ and magnitude ~15% of the saturated value occurring after ~2 decay times. The origin of this behavior is unclear presently and is the subject of further investigation.)

Based upon the pattern of light scattered at high fields, we can determine that the tubules align with their long axes parallel to the field direction. Since the lipid molecules that comprise the tubules are assumed to orient approximately perpendicular to the walls, the magnetic susceptibility anisotropy of the molecules must be <0, a result common to nearly saturated extended hydrocarbon chains (Boroske and Helfrich, 1978).

RESULTS AND ANALYSIS

A typical experimental run of Δn vs. H^2 for the concentration 0.17 mg/ml is shown by the data points in Fig. 3. Before proceeding with the full data analysis, we must first determine whether such a concentration is in the dilute regime, or whether we need to consider excluded volume effects. Based upon an Onsager (1949) formalism for long, hard rods taken to the level of the second virial coefficient, it can be shown (Photinos and Saupe, 1985; Rosenblatt and Zolty, 1985) that the Cotton–Mouton coefficient $C(\equiv d\Delta n/dH^2)$ scales as

$$C \propto \frac{\rho \Delta\alpha \Delta\chi}{\left(1 - \frac{\rho\pi d\ell^2}{16}\right)}, \tag{1}$$

where $\Delta\alpha$ is the polarizability anisotropy of the tubule, $\Delta\chi$ the volume magnetic susceptibility anisotropy, ρ the number density, d the tubule diameter, and ℓ the length. The tubules are hollow, having an average wall thickness of ~125 Å (2.5 bilayers), a diameter of 0.75 μm, and a length of 21 μm. Moreover, at a concentration of 0.17 mg/ml we find $\rho \approx 2.7 \times 10^8$ cm^{-3}. Thus the correction term $\rho\pi d\ell/16$ is ~0.018 which, given the experimental variation in the results, is not significant compared with 1. For this concentration, the sample can indeed be considered dilute and excluded volume interactions need not be considered further. (It is interesting to note that for appropriately shaped particles at high concentrations the Cotton–Mouton coefficient can be significantly enhanced, as shown by Lewis et al. [1985] who studied fragments of *H. halobium* [purple membrane] in the concentration region 1–11 mg/ml.) Finally, we note that other long range interactions such as van der Waals attractions are unlikely to play a significant role at multimicron separations, and therefore the only interaction considered is that of the field interacting with individual tubules.

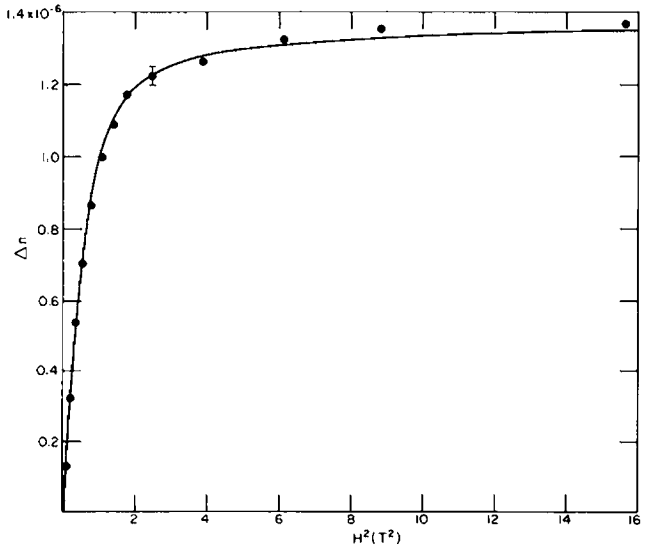

FIGURE 3 Δn vs. H^2. Solid line represents least squares fit to Eq. 4 when only the length distribution is considered.

To quantitatively interpret the measurements, we note that the sample birefringence is given by

$$\Delta n = \sum_{i=1}^{N} \Delta n_0 V_i \langle P_2(\cos\theta_i) \rangle, \tag{2}$$

where N is the number of tubules illuminated by the laser, Δn_0 the birefringence per volume of lipid, V_i is the volume of lipid in tubule i, and $P_2(\cos\theta_i)$ the second Legendre polynomial, i.e., $P_2(\cos\theta) = (3/2\cos^2\theta_i - 1/2)$, for tubule i having an orientation θ_i relative to the applied magnetic field. Note that the V-dependence in Eq. 2 remains valid even if form birefringence is important relative to intrinsic molecular birefringence, as long as the tubule walls are thin relative to their diameter, which is clearly the case here. Since it was earlier shown that the tubules are effectively nonmutually interacting, the only component to the orientational part of the free energy $\mathcal{F}_0$ depends upon the applied magnetic field: $\mathcal{F}_0 = -\Sigma_i (1/2)\Delta\chi V_i H^2 \cos^2\theta_i$ (DeGennes, 1975). Thus from $\mathcal{F}_0$ we obtain $\langle P_2(\cos\theta_i) \rangle$ by the Boltzmann distribution:

$$\langle P_2(\cos\theta_i) \rangle = \frac{\int_0^1 \left(\frac{3}{2}\cos^2\theta - \frac{1}{2}\right) \exp(\Delta\chi V_i H^2 \cos^2\theta / 2k_B T)\, d(\cos\theta)}{\int_0^1 \exp(\Delta\chi V_i H^2 \cos^2\theta / 2k_B T)\, d(\cos\theta)} \tag{3}$$

where k_B is the Boltzmann constant and T the temperature. Combining Eqs. 2 and 3, the birefringence can be written in closed form as

$$\Delta n = \sum_{i=1}^{N} \Delta n_0 V_i \left[\frac{3\sqrt{bV_iH^2} - D(\sqrt{bV_iH^2})}{4bV_iH^2 D(\sqrt{bV_iH^2})} - \frac{1}{2} \right] \tag{4}$$

where $b = \Delta\chi/2k_BT$ and Dawson's function $D(y)$ is defined as (Abramowitz and Stegvan, 1973)

$$D(y) = e^{-y^2} \int_0^y e^{t^2}\, dt. \tag{5}$$

From Eq. 4 we see that tubule volume has two effects: larger tubules (in terms of both length and wall thickness) with a larger susceptibility anisotropy ($\propto \Delta\chi\, V_i$) will have an orientational distribution more sharply peaked $\sim\theta = 0$; in addition, larger tubules contribute proportionally more ($\propto \Delta n_0 V_i$) to the birefringence. It is thus important to analyze the results in terms of the tubule size distribution, rather than assume a single average value for V. Such an analysis was earlier performed on purple membrane fragment data (Lewis et al., 1985), although in that case the fragment thicknesses were uniform and only the fragment area played a role in the distribution. For the case at hand, however, the situation may be complicated by the polydispersity in tubule wall thicknesses as well as in lengths, and thus it is important to perform several types of fits to the data.

For the first attempt we assumed an average wall thickness of 2½ bilayers (125 Å) and therefore a uniform cross sectional area A for the annulus of 2.9×10^{-10} cm^2. We then performed the summation in Eq. 4 over the length distribution in Fig. 1, where we substituted L_iA for V_i, such

that L_i is the length of tubule i. A two parameter ($\Delta n_0 \Sigma_i L_i A$, b) fit was performed to the data in Fig. 2 using Eq. 4 by summing over the 101 measured tubule lengths; the result is shown by the solid line in Fig. 3. For this particular experimental run, b was found to be -1.05×10^{13} T^{-2} cm^{-3}; taking $k_B T = 4.14 \times 10^{-14}$ erg, we thus find $\Delta\chi = -8.7 \times 10^{-1}$ erg cm^{-3} T^{-2}, which in cgs units is equal to $\Delta\chi = -8.7 \times 10^{-9}$ erg cm^{-3} G^{-2}. The magnitude of $\Delta\chi$ will be discussed later. At this point we note that the fit is only fair at best, with a strong systematic error. To more clearly see this, the quantity $\Delta n_{exper} - \Delta n_{calc}$ is plotted in Fig. 4. The open circles indicate that at both low and high fields the experimental values tend to lie above the fitted ("calc") curve, whereas at intermediate fields they fall below the fitted curve. Such behavior generally points toward a polydispersity that has yet to be taken into account; clearly we need to consider the distribution in wall thicknesses.

The wall thickness distribution is quantized in terms of the number of bilayers and is shown in Table II. The tubule fraction for 1, 2, and 3 bilayers is taken directly from the third column of Table I. For wall thicknesses of four or more bilayers, however, the data in Table I had to be interpolated in such a way that the total fraction in Table II sums to unity; we feel our interpolation is reasonable. Below we assume a thickness of 50 Å per bilayer (Rhodes, D. G., S. L. Blechner, P. Yager, and P. E. Schoen, manuscript in preparation). In principle the cross-sectional area A_i and tubule length L_i may be correlated, although we were unable to verify this from our optical and electron microscope measurements. For convenience, then, we assumed two totally uncorrelated distributions. In Eq. 4, V was rewritten as $L_i A_k$, and a double summation over the indices i and k was performed. Using this double distribution fitting procedure, b was found to be -8.5×10^{12} T^{-2} cm^{-3}, which in cgs units translates into $\Delta\chi = -7.0 \times 10^{-9}$ erg cm^{-3} G^{-2}. In performing the fit, moreover, no systematic deviation from the experimental results was evident, as seen by a plot of the data and least-squares fit in Fig. 5, as well as the quantity $\Delta n_{exper} - \Delta n_{calc}$ indicated by the solid points in Fig. 4. Note that the value of $\sqrt{\chi^2}$ for this fit was <1% of the full scale value, a number typical of most of the experimental runs. Another important point is the effect of the distribution interpolation used in Table II. If the fractions for 4–7 bilayers were divided differently, the ultimate results would change only slightly. For example, suppose the fraction for each of the four categories 4, 5, 6, and 7 bilayers were identical, i.e., 0.0265. In that case the resulting $\Delta\chi$ would be smaller than that found using Table II by only 2.5%. It turns out that Figs. 4 and 5 would also be virtually unchanged. Thus, the precise shape of the wall thickness distribution in the region for which there are few tubules is not extremely important. Additionally, a larger general drift of the baseline was also present. Since this drift tended to occur over long time scales, its effect was not to introduce scatter into the data but rather to introduce a larger run-to-run variation in the two fitted parameters. As a result, the experimental value of $\Delta\chi$ is taken to be $-7 \pm 1 \times 10^{-9}$ erg cm^{-3} G^{-2}. Finally, it is important to note the effects of a size distribution: by including the wall thickness distribution the fit was not only significantly improved, but the fitted value of $\Delta\chi$ was reduced by some 20%!

TABLE II
FRACTION OF TUBULES FOR EACH QUANTIZED WALL THICKNESS

Number of bilayers	Fraction
1	0.17
2	0.34
3	0.37
4	0.04
5	0.03
6	0.02
7	0.01
8	0.01
9	0.005
10	0.005

DISCUSSION

The value obtained for $\Delta\chi$ is of the same order of magnitude as values obtained for vesicles of egg lecithin (Boroske and Helfrich, 1978) and dimyristoyl lecithin (DMPC) bilayers (Scholz et al., 1984). In the former case Boroske and Helfrich obtained a cgs value of $\Delta\chi = -2.8 \times 10^{-9}$, by dynamic reorientation measurements in a magnetic field. Scholz et al., on the other hand, used a static technique measuring the orientational distribution function. Assuming a bilayer thickness of 60 Å, they found $\Delta\chi = -4.7 \times 10^{-9}$ for egg lecithin and -9.6×10^{-9} for DMPC. The larger value of the DMPC is not surprising, given that the tail is fully saturated. For the case at hand, although there are 17 methylene units per hydrocarbon chain, the polymerized tail structure contains both double and triple carbon–carbon bonds, whose susceptibility anisotropies are of opposite sign from that of a single bond (Schmalz et al.,

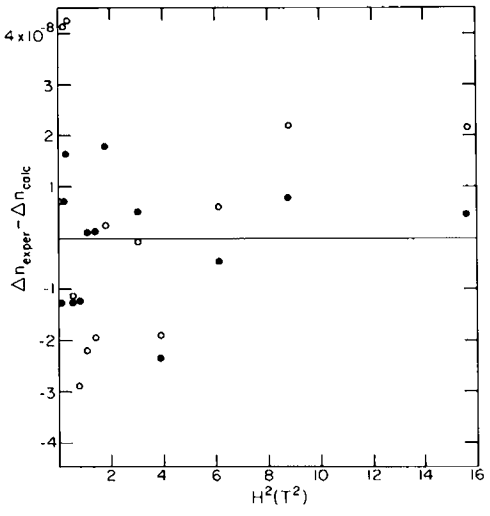

FIGURE 4 Difference between experimental and fitted values of Δn. Open circles include length distribution only, closed circles include both length and wall thickness distributions. Note that open circles exhibit a systematic deviation from experimental data.

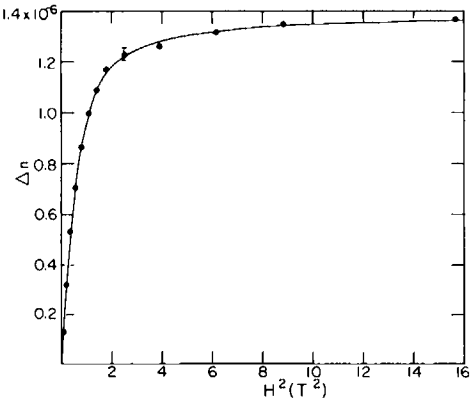

FIGURE 5 Δn vs. H^2. Solid line represents least-squares-fit to Eq. 4 when both length and wall thickness distribution are considered.

1973). Thus we would expect the magnitude of our measurement for $\Delta\chi$ to be smaller than that of DMPC.

The highly ordered tubule microstructure probably reflects, however, a regular crystal packing throughout its length, which differentiates it from most other biological lipid structures such as those above, that tend to be fluid, irregular, or polycrystalline. Here the tubules are probably similar to the platelet crystals of saturated-chain lecithins studied by Sakurai et al. (1980). If one makes the simple assumption that the molecular chain lies perpendicular to the bilayer surface, the measured values of $\Delta\chi$ go as $-1/2\ \rho s\Delta\chi_m$, where s is the number of molecules in the cylindrical part of the liposome and $\Delta\chi_m$ the molecular susceptibility anisotropy. The factor of $1/2$ arises from the approximately radial orientation of the individual molecules within the structure (Rosenblatt, 1986). The preceding analysis was based, however, upon the perhaps invalid assumption that the hydrocarbon chains, which contribute the most to the anisotropy, are perpendicular to the bilayer and the tubule axis. While in a fluid or polycrystalline bilayer the molecular long axes lie, on average, along the bilayer normal, they are in fact tilted (in such systems as saturated chain phosphatidylcholines) at 30° or more (Janiak et al., 1976). There is circumstantial evidence that the tubule wall consists of lipids with long-range order, and each monolayer may in fact be a single oriented crystal. If this were so, the particular chain packing in that crystal would have a substantial effect on the tendency of the tubules to orient in the field. As an extreme example, if the hydrocarbon chains were oriented in the plane of the bilayer and parallel to the tubule axis, the tubules would orient perpendicular to the field, whereas if the chains were oriented along tangents to the circumference, the tubules would orient along the field lines as observed. In other words, the degree and direction of orientation of a cylindrical microstructure in the field is a function of the polar angle ϕ between the hydrocarbon chain and the long axis, but not of the rotation of the chains about an axis parallel to the cylinder. One can in fact, easily calculate the angle ϕ (neglecting the contribution of the head group) for which $\Delta\chi$ changes sign. In the cylindrical geometry $\Delta\chi = \rho s\Delta\chi_m(3/2\cos^2\phi - 1/2)$ (DeGennes, 1975), which vanishes when $\phi = \sin^{-1}\sqrt{2/3}$, or ~55°. (Note that this is equivalent to a 35° tilt with respect to the layer normal.) Also note that this equation reduces to the earlier form $\Delta\chi = -1/2\ \rho s\Delta\chi_m$ when $\phi = 90°$, i.e., when the molecules lie perpendicular to the tubule axis.

Evidence that the hydrocarbon chain packing is unusual in $DC_{23}PC$ does exist. The electron density normal to the $DC_{23}PC$ tubule bilayer has been determined by low angle x-ray scattering (Rhodes, D. G., S. L. Blechner, P. Yager, and P. E. Schoen, manuscript in preparation). The phosphate-to-phosphate distance in tubules was found to be only 49.5 Å, as compared with 48.8 Å found in the gel phase of dipalmitoyl phosphatidylcholine, which is seven methylene units shorter (Janiak et al., 1976). The chain-packing must therefore allow partial interdigitation of the chains, or tilting of the molecules at ~45° from the bilayer normal, or some combination of the two. Of course if the 45° tilt were along the tubule axis, the sign of $\Delta\chi$ would change, which is experimentally not the case. This indicates that if a large tilt were indeed present, it would be distributed uniformly in direction, or perhaps biased away from the tubule axis owing to a possible coupling with the curvature elasticity.

From the foregoing discussion it's clear that we cannot make an estimate of $\Delta\chi_m$ without further information. Perhaps more useful would be a calculation of $\Delta\chi_m$ based upon bond susceptibility anisotropies and molecular conformation probabilities. Armed then with a theoretical value for $\Delta\chi_m$, one can work backward and deduce structural information about the molecular orientation; this work is currently underway. Analogous structural studies of other biological materials have already been mentioned by several authors (Hong et al., 1971; Maret and Dransfeld, 1977; Seelig et al., 1985; Lewis et al., 1985, for example). In conjunction with other probes, it should be possible in the future to use magnetic orientation to compare the structures of tubules made from different lipids, assess the effects of interactions with small hydrophobic molecules such as anesthetics on the lipid structure, and monitor the changes in conformation of the lipid molecules that occur during polymerization. Furthermore, orientability allows the study of parts of the microstructure other than the lipid hydrocarbon chains. For example, it can be used not only to study the structure which is itself oriented, but any material that can be attached to the tubule in an ordered manner. One example is study of oriented membrane proteins by various techniques; magnetic resonance experiments are obvious first choices as the field is already provided by the experiment.

We thank Dr. Alok Singh and Barbara Herendeen for the synthesis of the lipid used in the work, Jacque Georger and Carol Davies for preparation and characterization of tubule samples, and Ronald R. Price for assistance with the electron microscopy. We particularly thank Dr. David G. Rhodes of the University of Connecticut for allowing use of his x-ray diffraction data before formal publication.

This work was partially supported by the Defense Advanced Research Projects Agency and by the National Science Foundation under cooperative agreement DMR-8511789 to the Francis Bitter National Magnet Laboratory.

Received for publication 15 December 1986 and in final form 10 April 1987.

REFERENCES

Abramowitz, M., and I. A. Stegun. 1972. Handbook of Mathematic Functions. National Bureau of Standards, Washington, D.C.

Albrecht, O., D. S. Johnson, C. Villaverde, and D. Chapman. 1982. Stable biomembrane surfaces formed by phospholipid polymers. *Biochim. Biophys. Acta.* 687:165–169.

Baughman, R. H., and R. R. Chance. 1978. Fully conjugated polymer crystals; solid state synthesis and properties of the polydiacetylenes. *Ann. NY Acad. Sci.* 313:705–725.

Boroske, E., and W. Helfrich. 1978. Magnetic anisotropy of egg lecithin membranes. *Biophys. J.* 24:863–868.

DeGennes, P. G. 1975. Physics of Liquid Crystals. Claredon Press, Oxford.

Gaffney, B. J., and H. M. McConnell. 1974. Effect of a magnetic field on phospholipid membranes. *Chem. Phys. Lett.* 24:310–313.

Georger, J. H., A. Singh, R. R. Price, S. M. Schurr, P. Yager, and P. E. Schoen. 1987. Helical and tubular microstructures formed by polymerizable phosphatidylcholines. 3. *Am. Chem. Soc.* In press.

Glucksman, M. J., R. D. Hay, and L. Makowski. 1986. X-ray diffraction from magnetically oriented solutions of macromolecular assemblies. *Science (Wash DC.).* 231:1273–1276.

Helfrich, W. 1973. Lipid bilayer spheres, deformation and birefringence in magnetic fields. *Phys. Lett.* 43A:409–410.

Hong, F. H., D. Mauzerall, and A. Mauro. 1971. Magnetic anisotropy and the orientation of retinal rods in a homogeneous magnetic field. *Proc. Natl. Acad. Sci. USA.* 68:D1283–1285.

Hupfer, B., H. Ringsdorf, and H. Schupp. 1981. Polyreactions in oriented systems, 21: polymeric phospholipid monolayers. *Makromol. Chem.* 182:247–253.

Janiak, M., D. M. Small, and G. G. Shipley. 1976. Nature of the thermal pretransition of synthetic phospholipids: dimyristoyl- and dipalmitoyllecithin. *Biochemistry.* 15:4575–4580.

Janiak, M., D. M. Small, and G. G. Shipley. 1979. Temperature and compositional dependence of the structure of hydrated dimyristoyl lecithin. *J. Biol. Chem.* 254:6068.

Johnston, D. S., S. Sanghera, M. Pons, and D. Chapman. 1980. Phospholipid polymers: synthesis and spectral characteristics. *Biochim. Biophys. Acta.* 602:57–69.

Leaver, J., A. Alonzo, A. A. Durrani, and D. Chapman. 1983. The physical properties and photopolymerization of diacetylene-containing phospholipid liposomes. *Biochim. Biophys. Acta.* 732:210–218.

Lewis, B. A., C. Rosenblatt, R. G. Griffin, J. Courtemanche, and J. Herzfeld. 1985. Magnetic birefringence studies of dilute purple membrane suspensions. *Biophys. J.* 47:143–150.

Londsdale, K. 1939. Diamagnetic anisotrophy of organic molecules. *Proc. R. Soc. Lond.* 171:541–568.

Lopez, E., D. F. O'Brien, and T. H. Whitesides. 1982. Structural effects on the photopolymerization of bilayer membranes. *J. Am. Chem. Soc.* 104:305–307.

Maret, G., and K. Dransfeld. 1977. Macromolecules and membranes in high magnetic fields. *Physica.* 86–88B:1077–1083.

Nakashima, N., S. Asakuma, and T. Kunitake. 1985. Optical microscopic study of helical superstructures of chiral bilayer membranes. *J. Am. Chem. Soc.* 107:509–510.

O'Brien, D. F., T. H. Whitesides, and R. T. Klingbiel. 1981. The photopolymerization of lipid-diacetylenes in biomolecular-layer membranes. *J. Polym. Sci. Polym. Lett. Ed.* 19:95–101.

Onsager, L., 1949. The effects of shape on the interaction of colloidal particles. *Ann. NY Acad. Sci.* 51:627–659.

Photinos, P., and A. Saupe. 1985. Cluster integral expansion of the Cotton-Mouton constant in suspensions. *Mol. Cryst.* 123:217–227.

Rosenblatt, C. 1984. Temperature dependence of the anchoring strength coefficient at a nematic liquid crystal-wall interface. *J. Physique.* 45:1087–1091.

Rosenblatt, C., and N. Zolty. 1985. Electrolyte effects on a nearby second order nematic-isotropic phase transition in a micellar liquid crystal. *J. Physique.* 46L:1191–1197.

Rosenblatt, C. 1986. Micellar shape distribution in the isotropic phase near a prolate-to-oblate nematic phase transition. *J. Physique.* 47:1097–1102.

Sakurai, I., Y. Kawamura, A. Ikegami, and S. Iwayanagi. 1980. Magneto-orientation or lecithin crystals. *Proc. Natl. Acad. Sci. USA.* 77:7232–7236.

Sakurai, I., T. Sakurai, T. Seto, and S. Iwayanagi. 1983. Lyotropic phase transitions in single crystals of L- and DL-diapalmitoylglycerophoscolines. *Chem. Phys. Lipids.* 32:1–11.

Schmalz, T. G., C. L. Norris, and W. H. Flygare. 1973. Localized magnetic susceptibility anisotropies. *J. Am. Chem. Soc.* 95:7961–7967.

Schoen, P. E., and P. Yager. 1985. Spectroscopic studies of polymerized surfactants: 1,2-bis(10,12-tricosadiynoyl)-sn-glycero-3-phosphocoline. *J. Polm. Sci. Polym. Phys. Ed.* 23:2203–2216.

Scholz, F., E. Boroske, and W. Helfrich. 1984. Magnetic anisotropy of lecithin membranes. *Biophys. J.* 45:589–592.

Seelig, J., F. Borle, and T. A. Cross. 1985. Magnetic ordering of phospholipid membranes. *Biochim. Biophys. Acta.* 814:195–198.

Singh, A., and J. M. Schnur. 1985. Polymerized diacetylenic phosphatidylcholine vesicles: synthesis and characterization. *Polym. Preprint.* 26:184–185.

Singh, A., R. Price, J. M. Schnur, P. E. Schoen, and P. Yager. 1986. Tubule formation by heterobifunctional polymerizable lipids: synthesis and characterization. *Polym. Preprint.* 27:393–4.

Singh, A., B. P. Gaber, B. P. Singh, R. R. Price, T. G. Burke, P. E. Schoen, J. M. Schnur, and P. Yager. 1987. Synthesis and characterization of positional isomers of 1,2-bis ehptacosadiynoyl phosphatidylcholines *In* Surfactants in Solution. K. L. Mittal, editor. Elsevier, New York. In press.

Yager, P., and W. L. Peticolas. 1982. The kinetics of the main phase transitions of aqueous dispersions of phospholipids induced by pressure jump and monitored by Raman spectroscopy. *Biochim. Biophys. Acta.* 688:775–785.

Yager, P., J. P. Sheridan, and W. L. Peticolas. 1982. Changes in size and shape of liposomes undergoing chain melting transitions as studied by optical microscopy. *Biochim. Biophys. Acta.* 693:485–491.

Yager, P., and P. E. Schoen. 1984. Formation of tubules by a polymerizable surfactant. *Mol. Cryst. Liq. Cryst.* 106:371–381.

Yager, P., P. E. Schoen, C. Davies, R. Price, and A. Singh. 1985. Structure of lipid tubules formed from a polymerizable lecithin. *Biophys. J.* 48:899–906.